

Article

Evaluation of Eco-Friendly Hemp-Fiber-Reinforced Recycled HDPE Composites

Eleftheria Xanthopoulou ¹, Iouliana Chrysafi ², Prodromos Polychronidis ¹, Alexandra Zamboulis ^{1,*}
and Dimitrios N. Bikiaris ^{1,*}

¹ Laboratory of Polymer Chemistry and Technology, Department of Chemistry, Aristotle University of Thessaloniki, GR-541 24 Thessaloniki, Greece

² School of Physics, Aristotle University of Thessaloniki, GR-541 24 Thessaloniki, Greece

* Correspondence: azampouli@chem.auth.gr (A.Z.); dbic@chem.auth.gr (D.N.B.);
Tel.: +30-231-099-7812 (D.N.B.)

Abstract: The exploitation of natural fibers to reinforce polymers is a promising practice. Thus, biocomposites have gained increased attention in automotive, construction, and agricultural sectors, among others. The present work reports the reinforcement of recycled high-density polyethylene (r-HDPE) with hemp fibers to afford composite materials as sustainable analogues to conventional wood/plastic composite (WPC) products. HDPE bottles (postconsumer waste) were used as r-HDPE and further reinforced by the addition of hemp fibers. For the synthetic part, thirteen composite materials with different filler concentrations (10–75% wt. in hemp fibers) using either Joncryl or polyethylene-grafted maleic anhydride (PE-g-MA) as compatibilizers were prepared via melt mixing. Materials with good integrity were obtained with a fiber load as high as 75% wt. The structural, thermal, mechanical, and antioxidant properties of the r-HDPE/hemp composites were evaluated using multiple complementary characterization techniques. Stereoscopic microscope images demonstrated the satisfactory dispersion of the hemp fibers into the polymeric matrix, while scanning electron microscopy microphotographs revealed an improved adhesion between the filler and the polymeric matrix in the presence of compatibilizers. The incorporation of hemp fibers contributed to the improvement of the elastic modulus of the composites (almost up to threefold increase). The results showed that as the hemp fiber content increased, the antioxidant properties as well as the degradability of the composites increased. It is noteworthy that composites containing 75% wt. hemp fibers neutralized 80% of 2,2-diphenyl-1-picrylhydrazyl radicals within 45 min (DPPH assay). In conclusion, the present research work demonstrates that thermally recycled HDPE reinforced with biomass fibers received from agricultural waste is a valid alternative for the preparation of commodity products with an eco-friendly character compared to conventional wood/plastic composites.

Keywords: polymer recycling; composites; hemp fibers; sustainability; recycled HDPE



Citation: Xanthopoulou, E.; Chrysafi, I.; Polychronidis, P.; Zamboulis, A.; Bikiaris, D.N. Evaluation of Eco-Friendly Hemp-Fiber-Reinforced Recycled HDPE Composites. *J. Compos. Sci.* **2023**, *7*, 138. <https://doi.org/10.3390/jcs7040138>

Academic Editor: Francesco Tornabene

Received: 2 March 2023

Revised: 18 March 2023

Accepted: 31 March 2023

Published: 4 April 2023



Copyright: © 2023 by the authors. Licensee MDPI, Basel, Switzerland. This article is an open access article distributed under the terms and conditions of the Creative Commons Attribution (CC BY) license (<https://creativecommons.org/licenses/by/4.0/>).

1. Introduction

The disposal of plastic wastes in terrestrial and aquatic habitats along with the insufficient waste management constitute a significant environmental, financial, and social threat [1–3]. This problem was severely intensified during the COVID-19 pandemic, when tons of single-use polymeric materials, such as gloves and masks, were used on a daily basis [4,5]. Within this frame, European Union has established a policy to promote circular economy with the recycling of common petroleum-sourced polymers, such as high-density polyethylene (HDPE) [6] and poly(ethylene terephthalate) (PET) [7,8]. Furthermore, researchers are developing new technologies and processes to enhance their recycling and upcycling efficiency, such as thermomechanical processing, chemical recycling (glycolysis and pyrolysis), and biological depolymerization using enzymes and microorganisms [9,10].

Fiber-reinforced plastics/polymers (FRP) are well-known, commercially available composites, typically composed of a polymer matrix (usually a resin) reinforced with

fibers (e.g., glass or synthetic fibers). The incorporation of natural fibers [11–14], and more generally natural fillers [15,16], into polymeric matrices is an alternative strategy to obtain novel, environmentally friendly materials with improved properties and higher biobased and/or biodegradable content. Bast fibers, which are typically evaluated as reinforcing agents for polymer matrices [17,18], are commonly obtained from the outer cell stem's layers of several plants, mainly flax, jute, kenaf, and hemp. Some of the most desirable characteristics of natural fibers are their low density and specific weight, acceptable strength, toughness and stiffness, and biodegradability, accompanied, of course, by their green character [19,20].

Hemp fibers (HF) are one of the dominant classes of bast fibers, commonly isolated from the hemp plant (*Cannabis sativa* L.) [21–25]. The common features of natural fibers along with the inherent mechanical, thermal, and acoustic properties [26] of hemp fibers render them promising components for reinforcements in polymer composite materials [27–30]. Since hemp fibers are waste from the agricultural industry, they are inexpensive and available in important quantities, thus lowering the cost of the final products [31,32]. Consequently, the revalorization of by-products from industries or agroforestry to prepare composites similar to wood/plastic composites (WPC) supports the circular economy and creates a path for sustainability [33].

The biggest challenge in the preparation of composite materials is the successful interface adhesion between the filler and the polymer matrix. Within a composite, the mechanical as well as thermal properties depend on the characteristics of the matrix, the reinforcement, and their bond strength, which ensures proper orientation and positioning of the reinforcement, uniform transfer of load among the fibers, and resistance to damage and crack propagation [34–36]. When it comes to natural fibers, compatibilization and adhesion with the polymer matrix are even more challenging due to the highly hydrophilic nature of the fibers, composed mainly of cellulose and lignin, compared to the polymeric matrix, which is rather hydrophobic, especially in polyolefins [37]. Therefore, surface modification of the fibers and/or the polymer is a currently an active field of research in polymeric composites with natural fibers. There are, of course, other limitations linked to the use of natural fillers, such as the intrinsic variability of all bio-based compounds, higher moisture absorption, lower thermal stability, lower durability, lower fire resistance, etc.; nevertheless, the main difficulty remains obtaining satisfactory adhesion.

In the case of hemp fibers, chemical treatment, such as treatment with alkali, silanization, or surface-initiated polymerization [38–43], as well as physical treatments such as stretching, thermotreatment, and electric discharge have been proposed and studied as possible means to ameliorate the adhesion with the polymeric matrix [44–46]. In addition, polymer modification through reactive group grafting appears to be an effective process to offer better interfacial adhesion, without requiring solvent-based techniques [47–49]. Despite numerous studies, effective adhesion between natural fibers, hemp fibers included, and polyolefin matrices is still elusive.

Compared to fiber pre-treatment, which requires additional steps before the incorporation of fibers in the composites, the direct use of compatibilizers during the melt mixing process is a quite straightforward strategy. Within this context, polyethylene-grafted maleic anhydride (PE-g-MA) has been introduced as an effective compatibilizer. Active PE-g-MA groups can react with the surface hydroxyl groups of natural lignocellulosic fibers to generate chemical bonding between the polymer chain and the fiber and thus improve the final reinforcement of the matrix [50–54]. Joncryl[®] ADR 4400 is a patented, multi-functional polymeric chain extender with a medium epoxy equivalent weight (medium number of epoxy groups per chain) which can be used to improve the processing during extrusion of films, sheets, foams, paper coatings, and blow-molded objects, and constitutes an alternative option for polyolefins [55–57]. To the best of our knowledge, Joncryl has not been used for the compatibilization of natural fibers with HDPE.

Herein, a series of recycled high-density polyethylene (r-HDPE) hemp fiber composite materials, using Joncryl (JC) and PE-g-MA as compatibilizers, were prepared via

reactive extrusion (melt mixing). Pultrusion is regularly employed for the preparation of fiber-reinforced polymers [58]; nevertheless, it is typically applied to resins rather than thermoplastic polymers [59]. Melt mixing, another widely used process in the polymer industry [60], was employed for the preparation of the composites in the present study. Apart from the compatibilizer, we investigated a wide range of fiber contents, as high as 75% wt. The structural, thermal, and mechanical properties of the final polymers were investigated, implementing multiple techniques. Furthermore, their antioxidant activity was evaluated. Finally, soil degradation tests were conducted to exhibit the green profile of the composites.

2. Materials and Methods

2.1. Materials

r-HDPE was prepared from used bottles which were collected, shredded, and milled using a sieve of 1 mm diameter. Hemp fibers were supplied from KANNABIO (Volos, Greece). Polyethylene-grafted maleic anhydride (PE-g-MA) containing 0.5 wt. % maleic anhydride was purchased from Sigma-Aldrich. The polymeric chain extender Joncryl ADR[®] 4400, in the form of flakes, was supplied by BASF (Ludwigshafen, Germany). It has an epoxy equivalent weight of 485 g/mol and a weight-average molecular weight of 7100 g/mol. All other solvents and materials used were of analytical grade.

2.2. Preparation of the R-HDPE/Hemp Fibers Composites

The composite materials were prepared by melt mixing in a Haake–Buchler Reomixer (model 600) with roller blades and a mixing head with a volumetric capacity of 69 cm³. r-HDPE composites containing 10, 20, 50, and 75% wt. hemp fibers of 0.5 cm average length and 40 μm average diameter were prepared. Polyethylene-grafted maleic anhydride (PE-g-MA) or Joncryl ADR[®] 4400 were used as compatibilizers. The amount of compatibilizer was calculated according to the content of hemp fibers: 1% wt. based on the mass of hemp fibers (see Table 1 for detailed quantities).

Table 1. Composition of the prepared materials detailing the amounts of recycled high-density polyethylene (r-HDPE), hemp fibers (HF), polyethylene-grafted maleic anhydride (PE-g-MA), or Joncryl ADR[®] 4400 (JC) used.

Sample	r-HDPE (g)	Hemp Fibers (g)	Compatibilizer (g)	
			PE-g-MA	JC
r-HDPE neat		-	-	-
r-HDPE + 20% wt. HF	8	2	-	-
r-HDPE + 50% wt. HF	5	5	-	-
r-HDPE + JC	10	-	-	0.1
r-HDPE + 10% wt. HF + JC	9	1	-	0.1
r-HDPE + 20% wt. HF + JC	8	2	-	0.2
r-HDPE + 50% wt. HF + JC	5	5	-	0.5
r-HDPE + 75% wt. HF + JC	2.5	7.5	-	0.75
r-HDPE + PE-g-MA	10	-	0.1	-
r-HDPE + 10% wt. HF + PE-g-MA	9	1	0.1	-
r-HDPE + 20% wt. HF + PE-g-MA	8	2	0.2	-
r-HDPE + 50% wt. HF + PE-g-MA	5	5	0.5	-
r-HDPE + 75% wt. HF + PE-g-MA	2.5	7.5	0.75	-

r-HDPE, hemp fibers, Joncryl D4400, and PE-g-MA were dried at 60 °C under vacuum for 24 h prior to melt mixing in order to remove the adsorbed moisture. Appropriate amounts of r-HDPE, hemp fibers, and compatibilizer (Table 1) were fed into the Reomixer at 185 °C. A torque speed of 30 rpm was applied and the melt mixing process was carried out for 5 min. During the mixing period, the melt temperature and torque were continuously recorded. Materials were received in bulk and used as such. When necessary, specimens of appropriate shape were formed by thermal compression (Paul-Otto Weber (Germany) thermal press).

2.3. Characterization

2.3.1. Stereoscopic Microscopy

All the samples were observed through a stereomicroscope (SteREO Discovery V.20, Zeiss, Germany) equipped with a camera (GRYPHAX Altair, Jenoptik, Jena, Germany).

2.3.2. Attenuated Total Reflectance (ATR)

ATR measurements were performed in order to examine the chemical structure of the composites. ATR spectra were recorded on a Cary 670 spectroscope from Agilent Technologies (Palo Alto, CA, USA) equipped with a diamond-attenuated total reflectance (ATR) accessory (GladiATR, Pike Technologies, Madison, WI, USA). Infrared absorbance spectra were collected in the range from 4000 to 450 cm^{-1} using a resolution of 4 cm^{-1} and 32 co-added scans. The presented spectra were further baseline-corrected and normalized.

2.3.3. X-ray Diffraction (XRD)

XRD was employed to study the semi-crystalline structure of all samples at room temperature (RT) after having been melted. The XRD spectra were recorded by means of a MiniFlex II XRD system (Rigaku Co., Tokyo, Japan), with Cu Ka radiation (0.154 nm), over the 2θ range from 5° to 50° with a scanning rate of $1^\circ/\text{min}$.

2.3.4. Differential Scanning Calorimetry (DSC)

The thermal transitions of the synthesized materials were monitored using a differential scanning calorimeter (DSC) from Netzsch equipped with Intracooler (DSC Polyma 214), according to the following program: heating from RT to 190°C , and cooling at rate of $20^\circ\text{C}/\text{min}$ under nitrogen atmosphere.

2.3.5. Thermogravimetric Analysis (TGA)

In order to study the thermal degradation and the thermal stability of the samples during heating, a Labsys Evo 1100 thermogravimetric analyzer (TGA) was used. The samples were heated from room temperature (RT) to 600°C under 50 mL/min of nitrogen flow with a $20^\circ\text{C}/\text{min}$ heating rate. The samples were placed in alumina crucibles, while an empty alumina crucible was used as a reference. Prior to each sample's measurement, a blank experiment was conducted and subsequently was subtracted from the experimental curve to eliminate the buoyancy effect. Continuous recordings of sample temperature, sample weight, and its first derivative were collected.

2.3.6. Scanning Electron Microscopy (SEM)

SEM studies of films' surface were carried out using a JEOL JMS 7610 F (Freising, Germany) scanning microscope equipped with an energy-dispersive X-ray (EDX) Oxford ISIS 300 micro-analytical system. The samples were carbon-coated to ensure sufficient conductivity. Operating conditions were the following: accelerating voltage 10 kV, probe current 45 nA, and counting time 60 s.

2.3.7. Mechanical Properties

The tensile properties of the prepared composites were measured on an Instron 3344 dynamometer, in accordance with ASTM D638, using a crosshead speed of 5 mm min^{-1} . Relative thin sheets of about $350 \pm 25\ \mu\text{m}$ were prepared using an Otto Weber, Type PW 30 hydraulic press connected with an Omron E5AX Temperature Controller, at a temperature of $150 \pm 5^\circ\text{C}$. Dog-bone-shaped tensile test specimens (central portions $5 \pm 0.5\text{ mm}$ thick, 40 mm gauge length) were cut in a Wallace cutting press. The values of Young's modulus, elongation at break, and tensile strength were determined from at least five specimens.

Izod impact tests were performed using a Tinius Olsen apparatus in accordance with the ASTM D256 method.

2.3.8. Antioxidant Activity

The antioxidant activity of the samples was determined with the 2,2-diphenyl-1-picrylhydrazyl (DPPH) method, which was developed according to Blois in 1958 [61]. Each film of 0.5×1 cm was added to 3 mL of a 5×10^{-3} mg/mL DPPH/EtOH solution. The samples remained in the solution for 1, 2, 3, and 24 h and the absorbance of each solution was recorded with the aid of a UV-Vis spectrometer (UV Probe 1650, Shimadzu, Tokyo, Japan) at 515–517 nm. The free radical scavenging activity was calculated as reported by Brand et al. according to the following equation:

$$\text{Free Radical scavenging activity (\%)} = \frac{A_0 - A_1}{A_0} \times 100 \quad (1)$$

where A_0 (AU) is the absorbance of the control sample and A_1 (AU) is the absorbance of each solution.

2.3.9. Soil Degradation Tests

The biodegradability of the prepared composites in the soil was determined by measuring the mass loss of films of 0.5×1 cm and thickness of 0.4 ± 0.02 mm buried in conventional leaf mold. Each specimen was buried in the soil in plastic nets at room temperature (about 30 °C). Water was supplied every 5 days, and the soil was kept so as not to be dried. Each specimen was taken out of the soil after burial for 1, 2, 4, and 6 months. Obtained films were washed with distilled water and dried to a constant mass under vacuum at 50 °C. The degree of soil degradation was estimated by the sample weight loss, according to the following equation:

$$\text{Mass loss\%} = \frac{W_0 - W_i}{W_0} \quad (2)$$

where W_0 is the initial weight (g) of the film and W_i is the weight (g) after soil burial. Each experiment was performed in triplicate and the mean value was calculated.

3. Results and Discussion

3.1. Synthesis of Composite Materials

In total, thirteen composite materials were synthesized via the melt mixing procedure. The compositions of the prepared composites are summarized in Table 1.

After the synthesis of the desired composite materials, films of the resulting samples were prepared by compression molding. As illustrated in Figure 1, in the formed films, the dispersion of the hemp fibers seemed to be homogeneous, except from the r-HDPE + 75% wt. HF + JC. This can be attributed to the high percentage of the filler, along with insufficient blending before the melt mixing procedure. Moreover, the prepared films were characterized by similar thickness of 0.4 ± 0.02 mm, while the color of the composite films turned darker as the content in filler increased, due to the presence of the brown hemp fibers.

3.2. Stereoscopic Microscopy

An additional remark about the dispersion of the hemp fibers into the r-HDPE matrix could be added after the observation with the stereoscopic microscope. As Figure 2 shows, hemp fibers were homogeneously dispersed into the polymeric matrix owing to the compatibilizer effect. In other words, there were fibers distributed throughout the material. In general, the surface of the prepared films seemed to be smooth, whereas for the r-HDPE + 75% wt. HF samples, the surface of the composites revealed a more “wrinkled” character, attributed to the high content of hemp fibers.

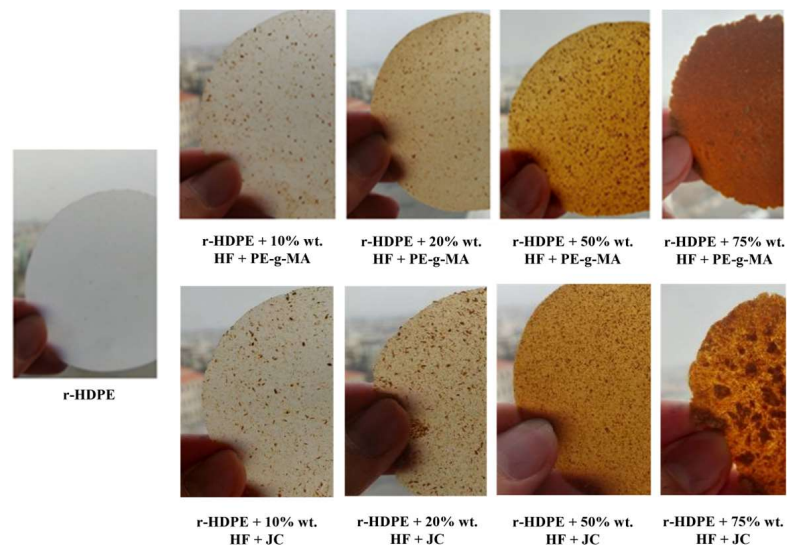


Figure 1. Illustration of recycled high-density polyethylene (r-HDPE) and r-HDPE + hemp fiber (HF) composite materials with different compatibilizers (polyethylene-grafted maleic anhydride (PE-g-MA) or Joncryl (JC)).

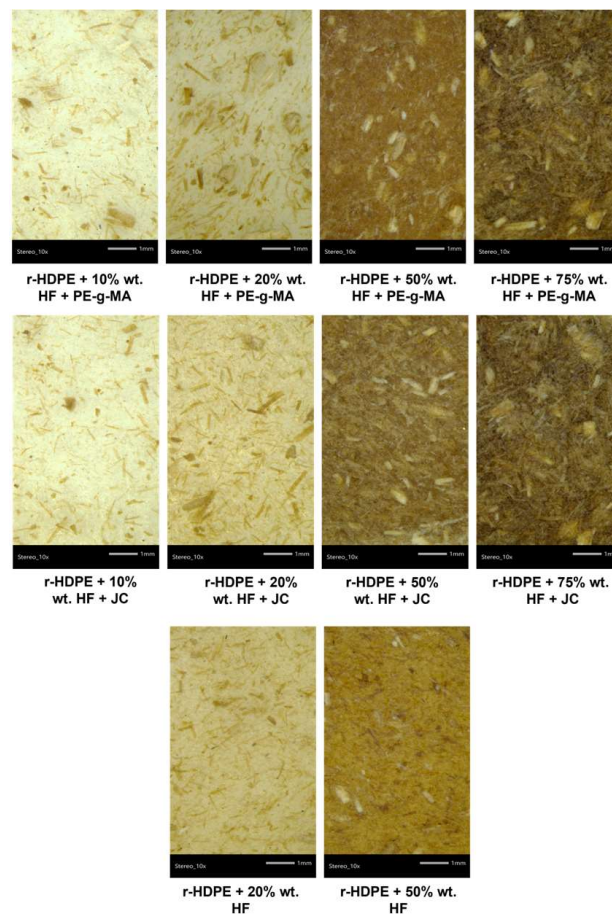


Figure 2. Stereoscopic microscope images for the recycled high-density polyethylene (r-HDPE) + hemp fibers (HF) composite materials.

3.3. Attenuated Total Reflectance (ATR)

ATR measurements were performed to verify the chemical structure of the r-HDPE + HF composites with the presence of a compatibilizer. As indicated by the Figure 3, the

composites revealed the same characteristic absorbance peaks with neat r-HDPE [62,63]. Particularly, regarding the main absorption peaks of HDPE in the range between 3000 and 2750 cm^{-1} , an intense double peak is observed, which is due to the asymmetric and symmetric stretching vibrations of the C-H bond (2919 cm^{-1} , 2847 cm^{-1}) in the $-\text{CH}_2-$ groups of r-HDPE. The main sharp peak at 1470 cm^{-1} is attributed to the C-H bending vibrations of the $-\text{CH}_2-$ groups of r-HDPE, while the peak at 716 cm^{-1} is due to the bending of the C-H bonds [64]. Concerning the hemp fiber composites, a small alteration, especially for the composite materials with the higher content in filler, can be noted around 1040 cm^{-1} ; the intensity of this peak increased as the content in the hemp fibers increased. The aforementioned band constitutes a characteristic one for hemp fibers and can be attributed to the bending vibration of the C–O–C bonds of pectin and cellulose [65].

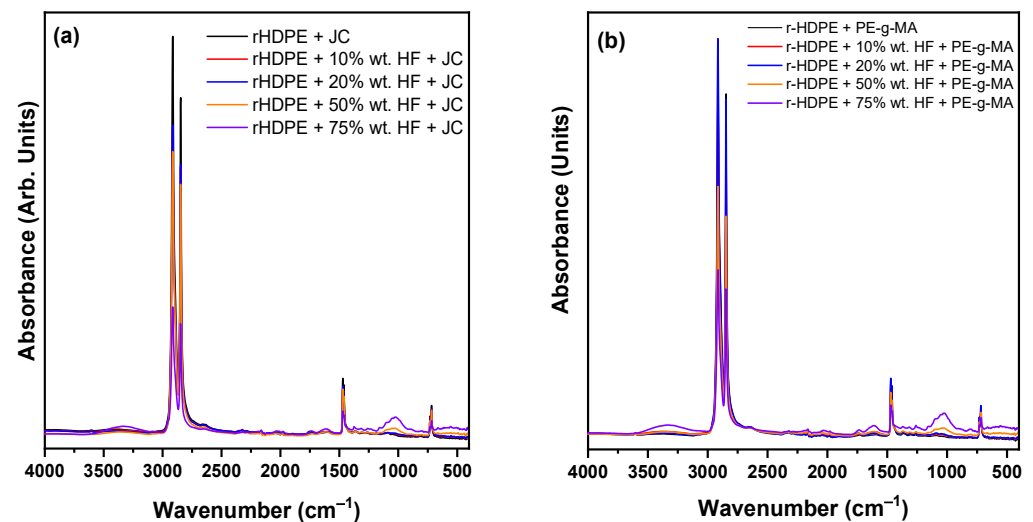


Figure 3. ATR spectra of the prepared (a) recycled high-density polyethylene (r-HDPE) + hemp fibers (HF) + Joncryl (JC), and (b) r-HDPE + HF + polyethylene-grafted maleic anhydride (PE-g-MA) composite materials.

3.4. X-ray Diffraction (XRD)

The crystalline state of r-HDPE composites with hemp fibers in different percentages, as well as with or without the addition of a compatibilizer, was studied with XRD. As it can be observed, in all cases, the characteristic crystalline diffraction peaks of the polymeric matrix associated with orthorhombic HDPE appear: 21.5° (110 plane) and 24.1° (200 plane) (Figure 4). The major diffraction peaks observed for hemp fibers at approximately 15.2° and 22.5° are attributed to cellulose and are more visible in the composites with higher hemp content [51]. In addition, in the composites, a shift in the HDPE diffraction peaks to smaller or higher 2θ values and their broadening is evident, which is attributed to the expected disruption of the arrangement of the polymer chains by the addition of the hemp fibers. As can be seen, this trend is more pronounced in the case of PE-g-MA. However, due to the large percentage of the additive in the final materials, it is difficult to estimate their effect on the degree of crystallinity of r-HDPE.

In a second phase, the patterns of the composite materials prepared without and with one of the two different compatibilizers were compared (Figure 4c,d). It can be seen that in both synthesized series, the final materials containing compatibilizer showed a lower degree of crystallinity, as well as a greater deviation from the diffraction peaks of r-HDPE. In addition, it was observed that the characteristic broad diffraction peak of hemp fibers appeared at a higher intensity in the compatibilized final materials.

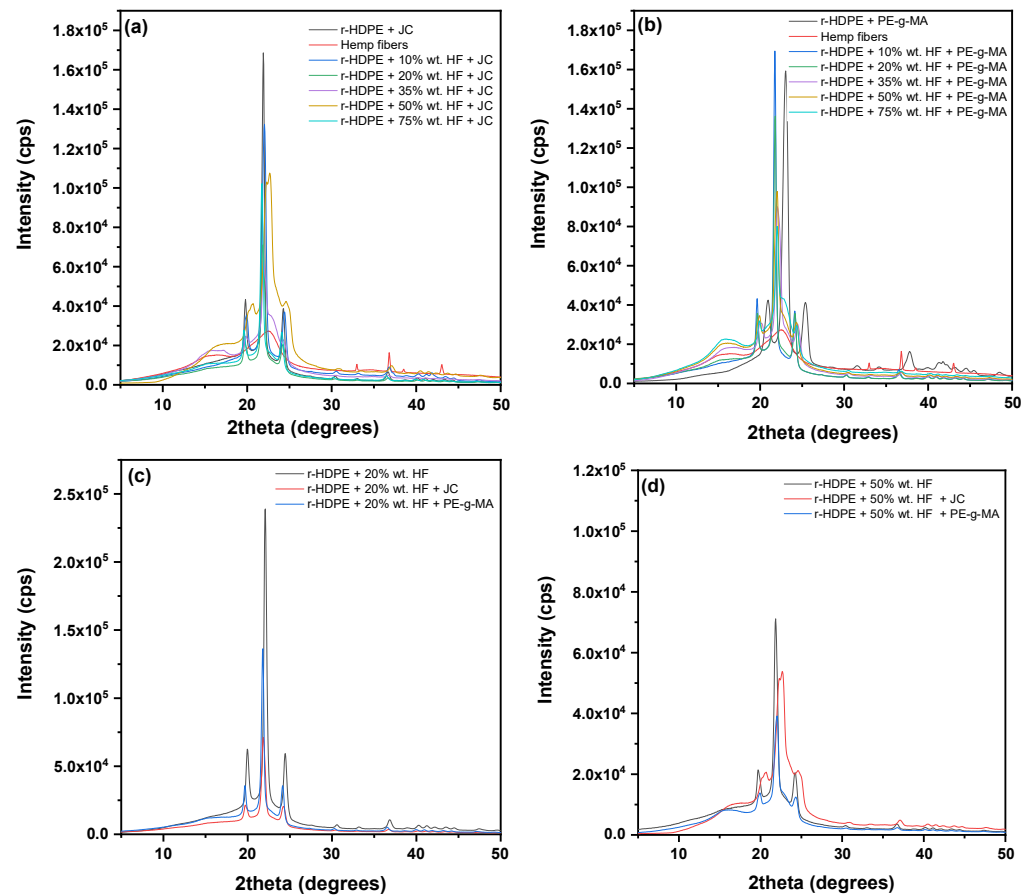


Figure 4. Comparative XRD patterns of the prepared (a) recycled high-density polyethylene (r-HDPE) + hemp fibers (HF) + Joncryl (JC), (b) r-HDPE + HF + polyethylene-grafted maleic anhydride (PE-g-MA) composite materials, (c) r-HDPE + 20% wt. HF with different compatibilizers, and (d) r-HDPE + 50% wt. HF with different compatibilizers.

3.5. Differential Scanning Calorimetry (DSC)

DSC measurements were performed in order to study the effect of hemp fiber filler on the thermal properties of r-HDPE. The second heating and cooling cycles of the r-HDPE + HF composites are shown in Figure 5, and the main characteristic data are summarized in Table 2. The slight initial decrease in the crystallization temperature (T_c), followed by an increase with higher hemp fiber content, indicated that the incorporation of large and small amounts of filler disturbed and facilitated, respectively, the crystallization process of the r-HDPE, to some extent. This is in agreement with the XRD results, where small deviations and a broadening of peaks were observed for the composites compared to neat HDPE. Concerning the melting temperature of the composites, it seemed to be affected by the introduction of the fillers to a limited extent, since for all the composite materials, the melting temperatures are within the range 133.6–135.6 °C. However, the melting enthalpies for the composites varied after the incorporation of the fillers. This phenomenon could be ascribed to the diluting effect provoked by the introduction of the fibers, which decreased the amount of the polymeric chains that possibly could undergo thermodynamic transitions during melting processes [66].

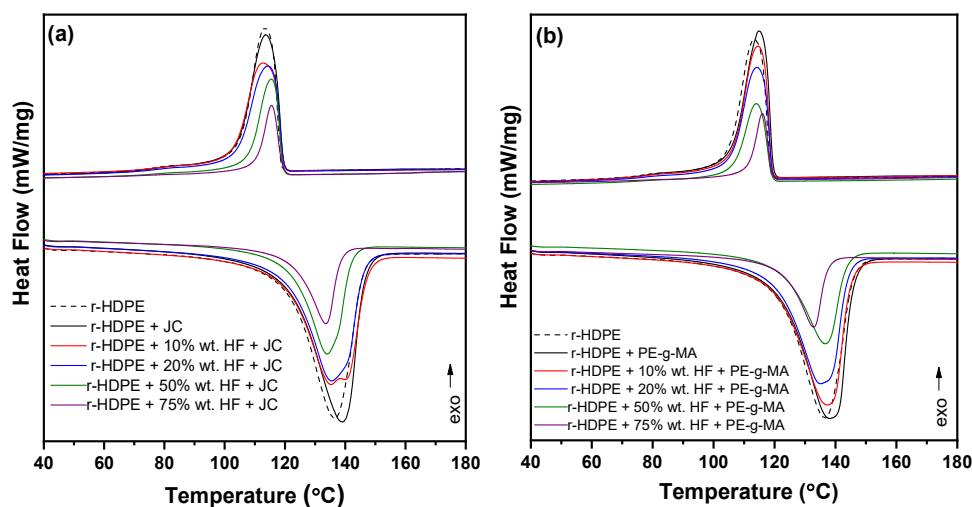


Figure 5. DSC thermograms of the prepared (a) recycled high-density polyethylene (r-HDPE) + hemp fibers (HF) + Joncryl (JC), and (b) r-HDPE + HF + polyethylene-grafted maleic anhydride (PE-g-MA) composite materials during the second heating and cooling scan.

Table 2. Summary of the thermal values (melting and crystallization temperatures) for recycled high-density polyethylene (r-HDPE) + hemp fibers (HF) composites.

Sample	Without Compatibilizer		+1% wt. JC		+1% wt. PE-g-MA	
	T _m (°C)	T _c (°C)	T _m (°C)	T _c (°C)	T _m (°C)	T _c (°C)
r-HDPE	136	113.5	139.1	113.6	138	114.9
r-HDPE + 10% wt. HF	-	-	135.3	112.7	137.3	114.5
r-HDPE + 20% wt. HF	136.9	114.2	135.6	114.4	136.1	114.3
r-HDPE + 50% wt. HF	134.2	115.2	134	115.5	136.7	114
r-HDPE + 75% wt. HF	-	-	133.6	115.5	132.8	116

3.6. Thermogravimetric Analysis (TGA)

The thermal stability and decomposition of r-HDPE composite materials with hemp fibers in the presence of compatibilizers were monitored using TGA. TGA was performed to gain insight on the maximum temperature at which the materials can be processed and further used.

The comparative thermograms of the mass loss and the derivative of the mass loss of r-HDPE and r-HDPE + 20 and 50% wt. HF with and without the addition of compatibilizers are presented in Figure 6. Regarding neat r-HDPE, it can be observed that the two compatibilizers accelerate the onset of the polymer’s degradation. The same trend was observed in the r-HDPE + 20 and 50% wt. HF samples.

Figure 7 shows the mass loss and mass loss derivative thermograms of r-HDPE and its composites with the addition of JC and PE-g-MA as compatibilizers. From the thermograms of mass loss, it can be clearly observed the existence of two stages of degradation, while another stage with a small mass loss is more evident as the percentage of hemp fibers increases between about 250 and 310 °C. In the presence of JC (Figure 7a), for the sample with 10% wt. hemp fibers, two stages of degradation with maximum rates at 354 °C (first stage) and at 494 °C (second/main stage) can be seen. As the percentage of fibers increases, another stage appears, as mentioned above, and is better distinguished in the diagram of the derivative of the mass loss (Figure 7b). It extends between the temperature range of 250 and 310 °C and is due to the decomposition of hemicellulose. The second stage extends up to 415 °C and is due to the decomposition of cellulose, while the percentage of mass that decomposes increases with the increase in the percentage of hemp [6]. In the main stage of degradation up to 600 °C, the complete decomposition of r-HDPE and a percentage of lignin is observed, while the mass that remains and increases with the increase in its

percentage is due to a small percentage of lignin that is not completely decomposed and other minerals. For reference, the remaining mass is 3%, 5%, 12%, and 15% for the samples with 10, 20, 50, and 75% wt. HF, respectively. Likewise, in the case of the addition of the PE-g-MA as stabilizer, three degradation stages have been presented (Figure 7c,d).

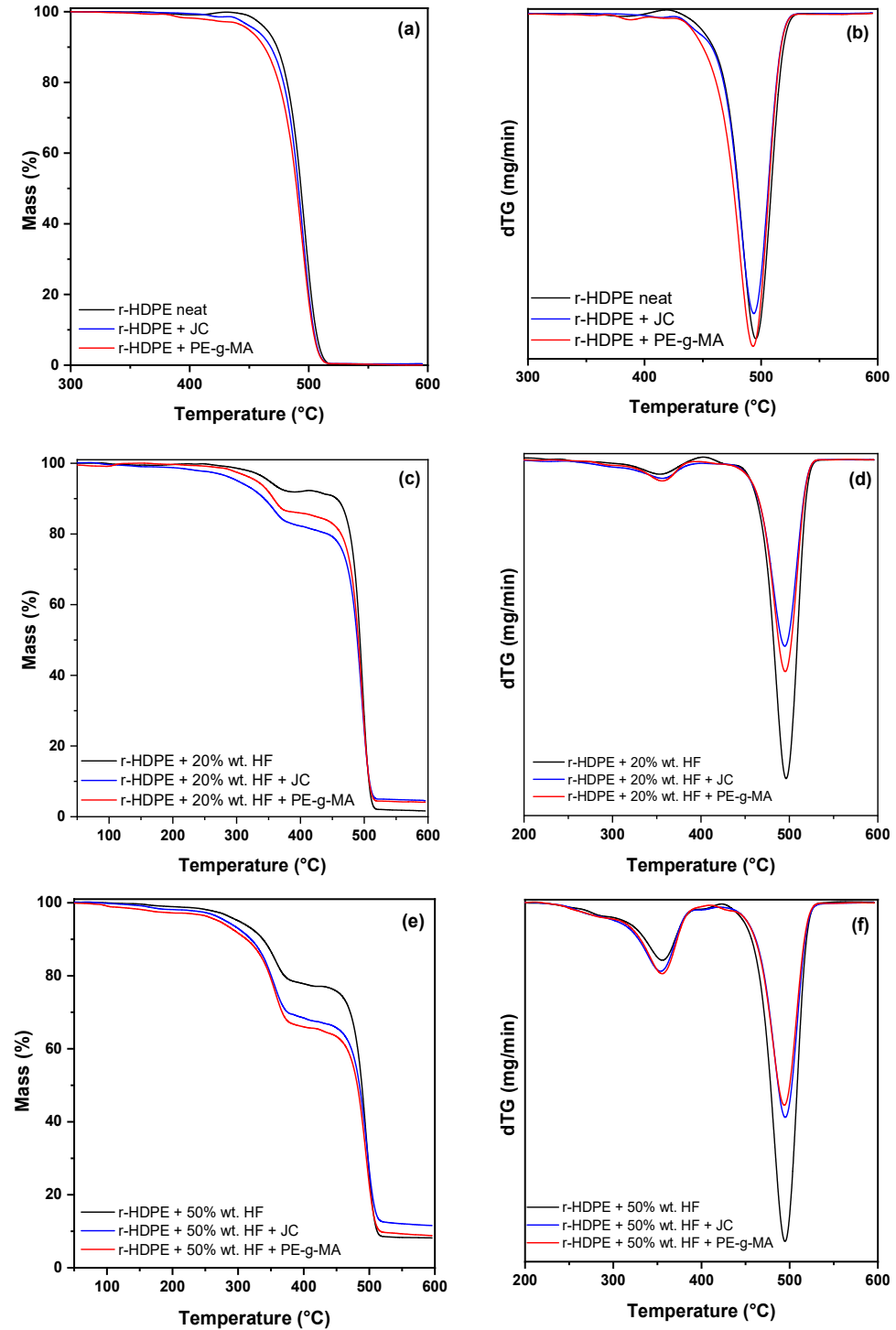


Figure 6. Comparative thermograms of the mass loss and the derivative of the mass loss of (a,b) recycled high-density polyethylene (r-HDPE), (c,d) r-HDPE + 20% wt. hemp fibers (HF), and (e,f) and 50% wt. HF.

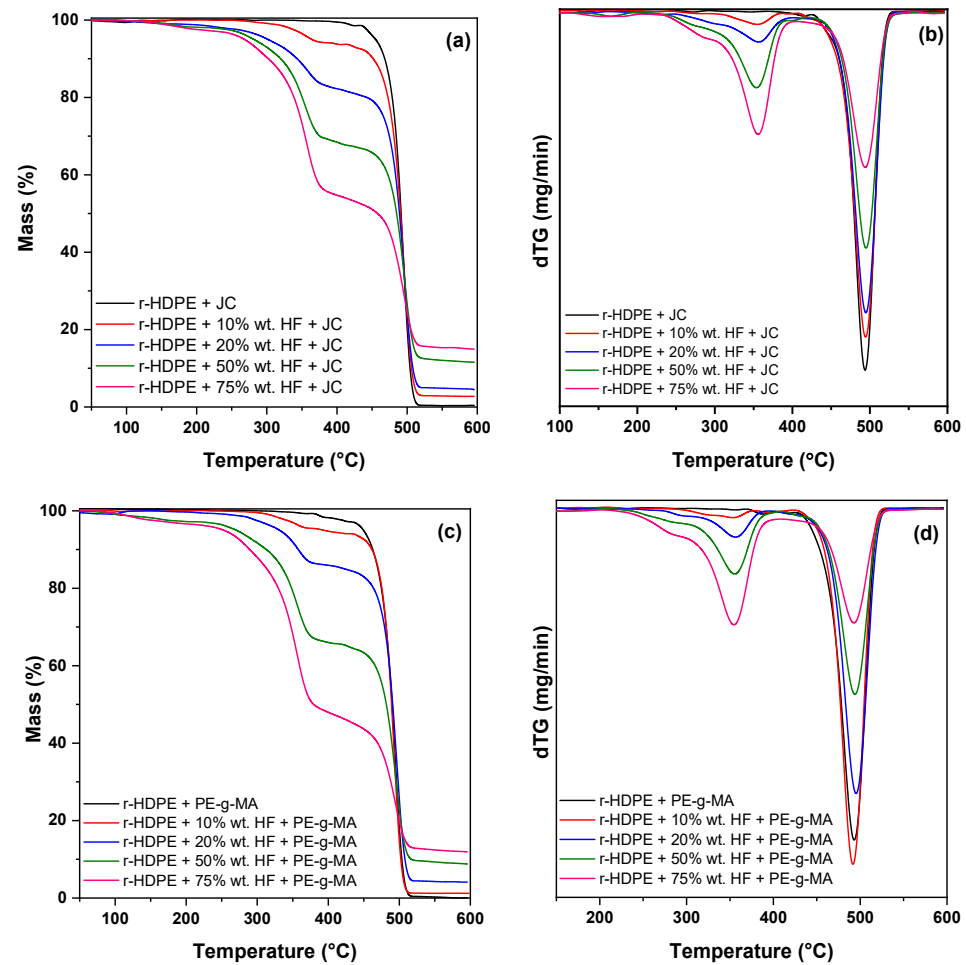


Figure 7. Comparative thermograms of the mass loss and the derivative of the mass loss of (a,b) recycled high-density polyethylene (r-HDPE) + hemp fibers (HF) + Joncryl (JC) and (c,d) r-HDPE + HF + polyethylene-grafted maleic anhydride (PE-g-MA) composite materials.

Figure 8 shows the plots of the thermal stability of the composites with respect to r-HDPE with the addition of the compatibilizers JC (Figure 8a) and PE-g-MA (Figure 8b). A downward trend in thermal stability is observed with both compatibilizers. The decrease in thermal stability in the presence of increasing amounts of hemp fibers is in accordance with the literature, and expected since natural fibers exhibit a much lower stability than the HDPE polymeric matrix. Moreover, the samples with the addition of 50 and 75% wt. of hemp fibers in the presence of the JC compatibilizer are more thermally stable than those with the PE-g-MA. This could be an indication of better adhesion in the presence of JC.

All in all, it is observed that the thermal degradation of the composites is affected by the incorporation of the hemp fibers. As seen, the composites with 50 and 75 wt% of hemp are pretty stable at temperatures until approximately 200 °C, while composites with lower content of hemp fibers are thermally stable until 200–250 °C. In other words, although thermal stability is lower than in r-HDPE, sufficient thermal stability is retained.

3.7. Scanning Electron Microscopy (SEM)

The study of the morphology of the composite materials and the dispersion of the additive in the final samples was carried out using SEM. The microphotographs of all materials are listed in Figures 9–11.

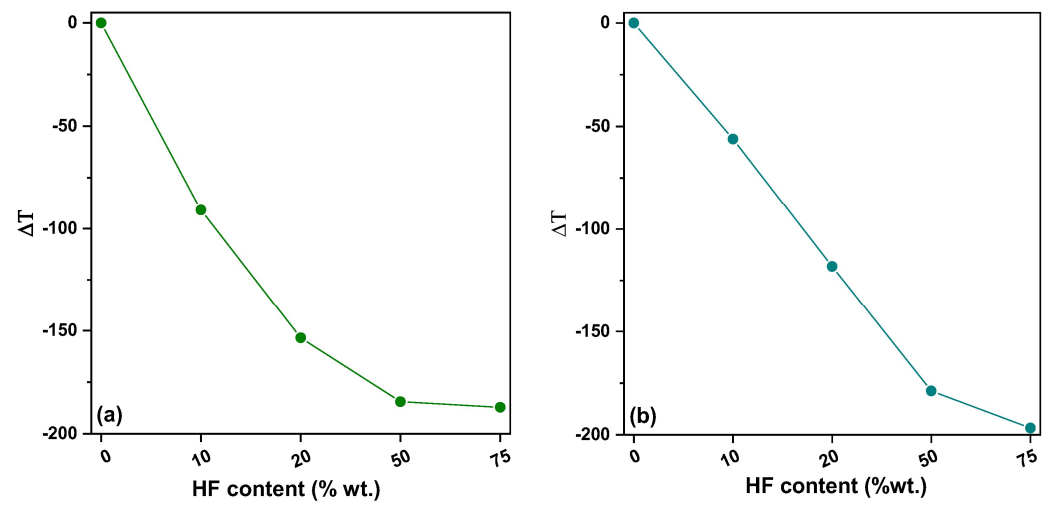


Figure 8. Plots of the thermal stability of the composites with respect to r-HDPE with the addition of the compatibilizers (a) Joncryl (JC), and (b) polyethylene-grafted maleic anhydride (PE-g-MA).

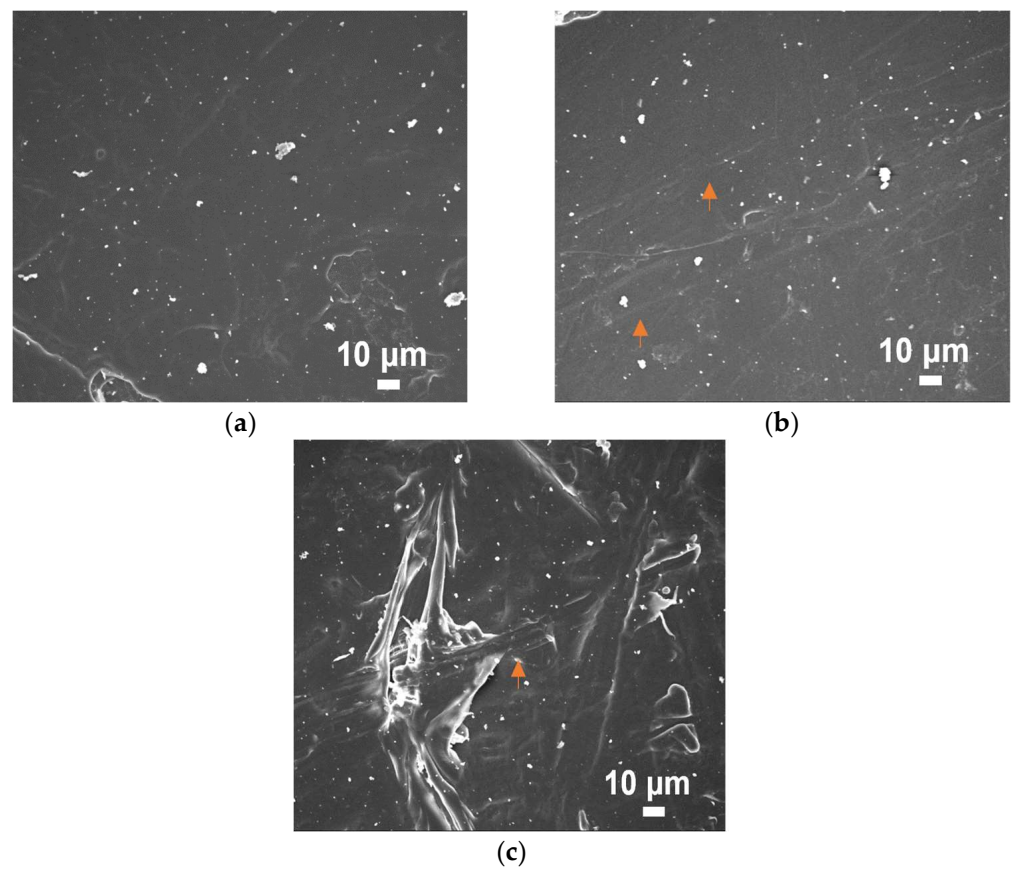


Figure 9. Microphotographs of (a) recycled high-density polyethylene (r-HDPE), and r-HDPE + (b) 20% wt. and (c) 50% wt. hemp fibers (HF) composite materials. Magnification $\times 500$.

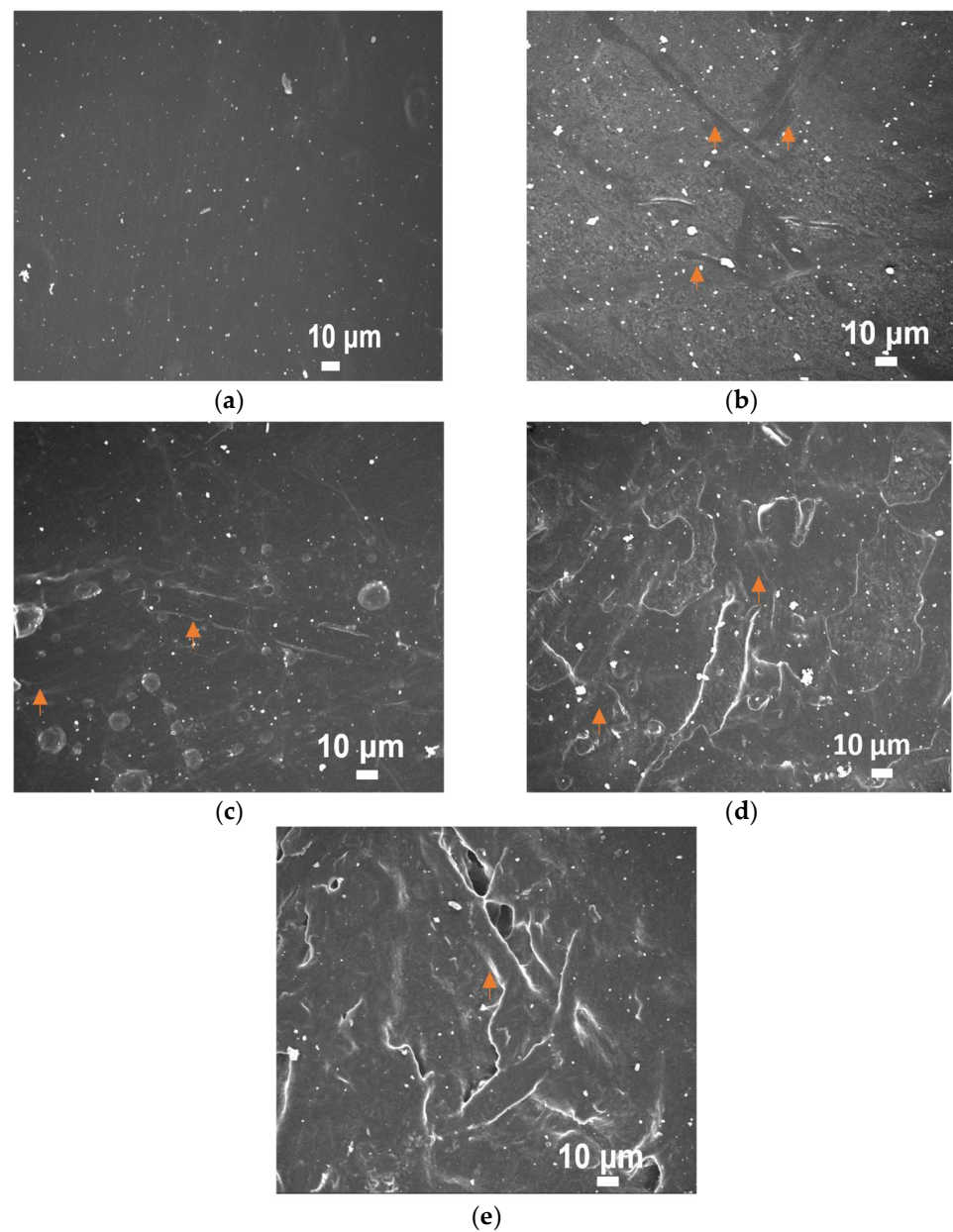


Figure 10. Microphotographs of (a) r-HDPE and r-HDPE + (b) 10% wt., (c) 20% wt., (d) 50% wt., and (e) 75% wt. HF + JC composite materials. Magnification $\times 500$.

More specifically, the composite materials produced without the use of compatibilizers are presented in Figure 9. As it can be seen, increasing the percentage of the additive has led to a greater disruption of the polymeric matrix. In addition, the presence of fibers both on the surface and in lower layers of the final material is evident (orange arrows). Finally, efficient dispersion of the additive is observed, a desirable feature in the preparation of composite materials.

The same trend is followed in the case of r-HDPE + HF composite materials with the presence of JC (Figure 10) and PE-g-MA (Figure 11) as compatibilizers. Specifically, an increase in the presence of the additive is observed, which agrees with the increase in hemp fibers in the feed. Furthermore, the existence of strongly bound fibers inside the r-HDPE is detected, which confirms the improved adhesion of the additive in the presence of compatibilizers.

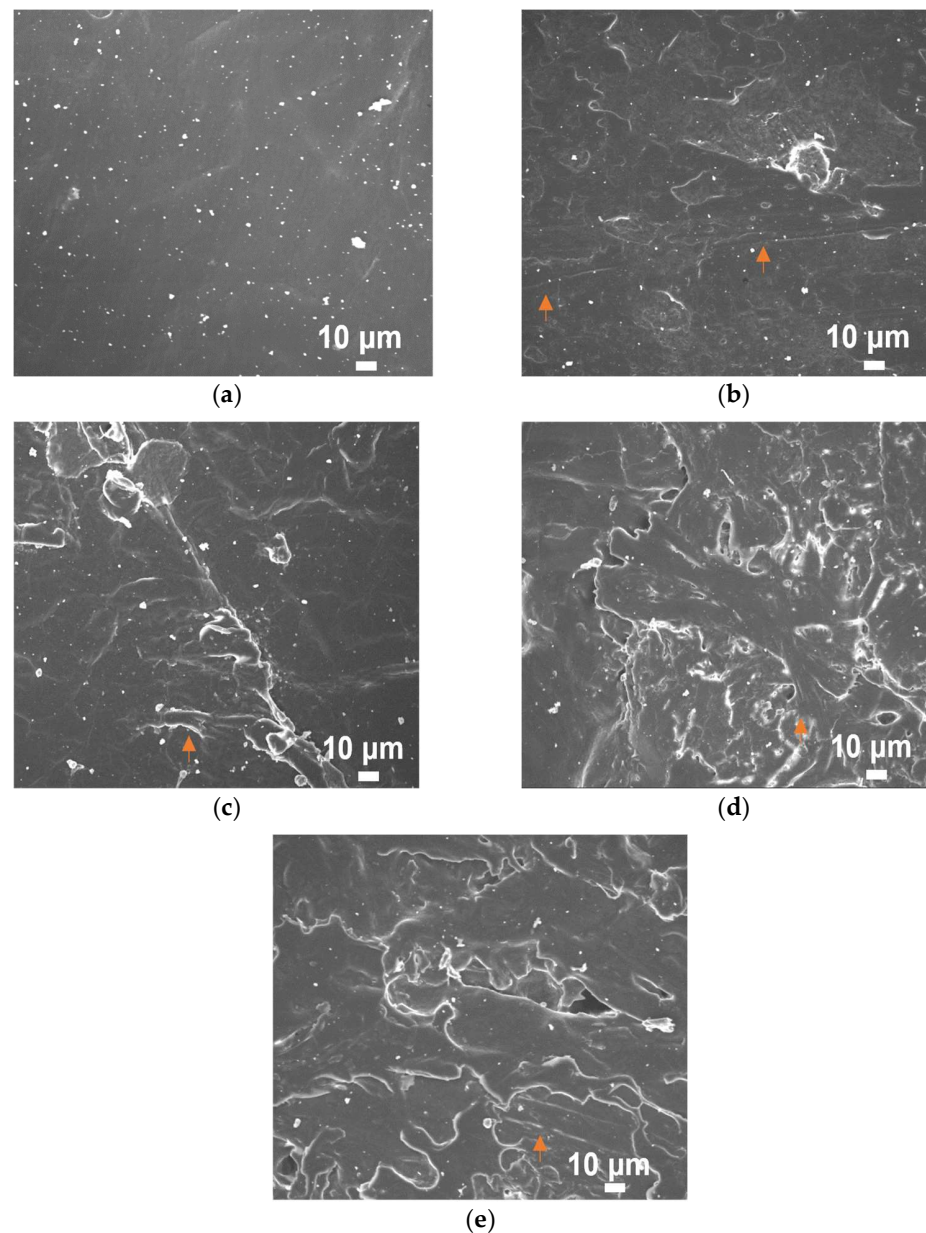


Figure 11. Microphotographs of (a) r-HDPE and r-HDPE + (b) 10% wt., (c) 20% wt., (d) 50% wt., and (e) 75% wt. HF + PE-g-MA composite materials. Magnification $\times 500$.

3.8. Mechanical Properties

3.8.1. Tensile Tests

The characteristic stress–strain curves of the r-HDPE + HF composites in the absence of a compatibilizer, as well as in the presence of the two different compatibilizers, are presented in Figure S1. In addition, the exact values of the parameters examined through the tensile strength measurements are listed in Tables S1–S3.

As it can be observed, the composite materials prepared with the addition of a compatibilizer have exhibited an improved Young's modulus value, in comparison with the corresponding neat composites, an encouraging fact for their subsequent application. More specifically, it is observed that in the materials r-HDPE + HF + JC, the modulus of elasticity increases with the increasing percentage of filler in the final composite (Figure 12).

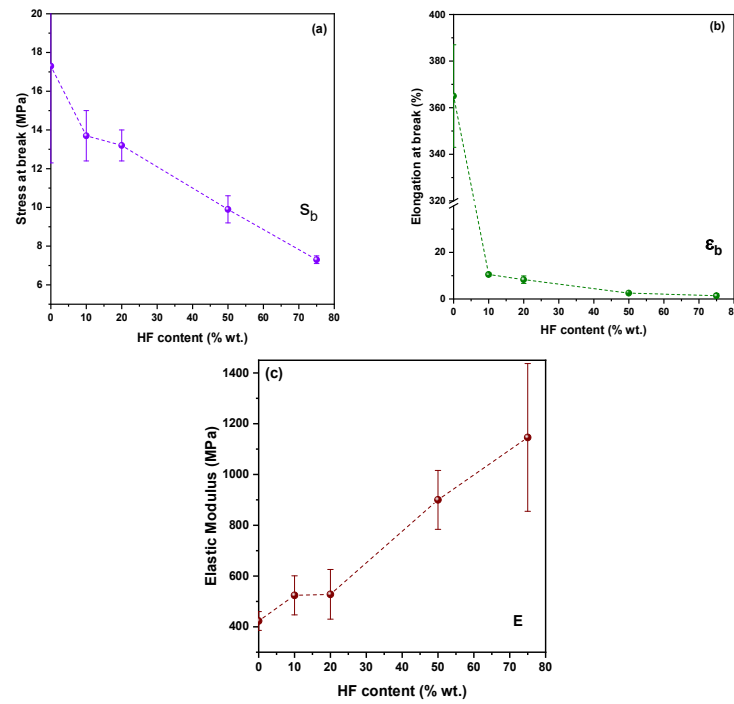


Figure 12. Effect of HF content on the (a) tensile stress at break, (b) elongation at break, and (c) elastic modulus of recycled high-density polyethylene (r-HDPE) + hemp fibers (HF) + Joncryl (JC) composite materials. The lines are drawn to guide the eye.

This trend also appears in the case of r-HDPE + HF + PE-g-MA materials (Figure 13). However, r-HDPE + 75% wt. HF + PE-g-MA shows a decreasing trend, which can be interpreted as a result of the creation of many crack points due to the high percentage of fibers in the polymer matrix.

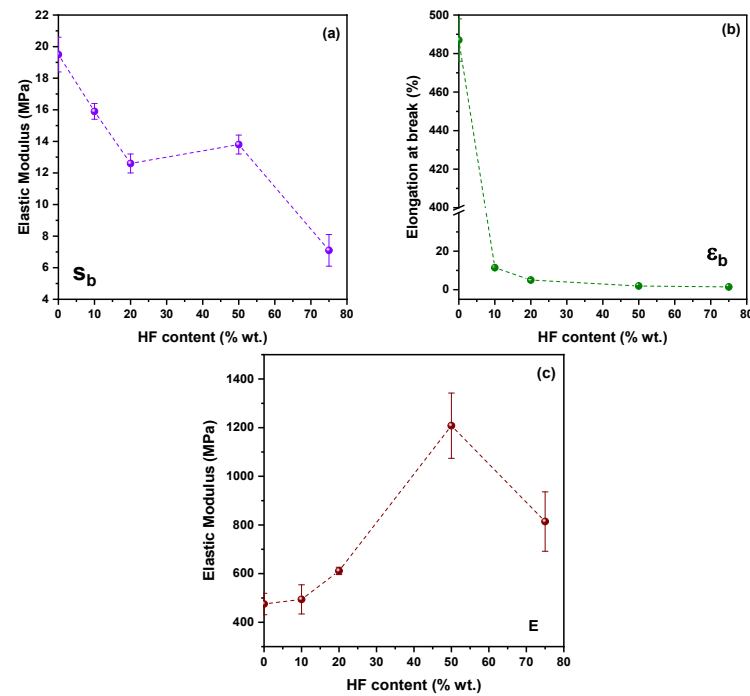


Figure 13. Effect of HF content on the (a) tensile stress at break, (b) elongation at break, and (c) elastic modulus of r-HDPE + HF + polyethylene-grafted maleic anhydride (PE-g-MA) composite materials. The lines are drawn to guide the eye.

3.8.2. Impact Strength

For further characterization of the mechanical properties, impact strength experiments were performed. The obtained values of each sample are illustrated in Figure 14. As it can be observed, the incorporation of HF resulted in lower impact strength values, compared to the neat HDPE. The addition of JC as a compatibilizer led to materials with increased values in comparison with those that were prepared using PE-g-MA.

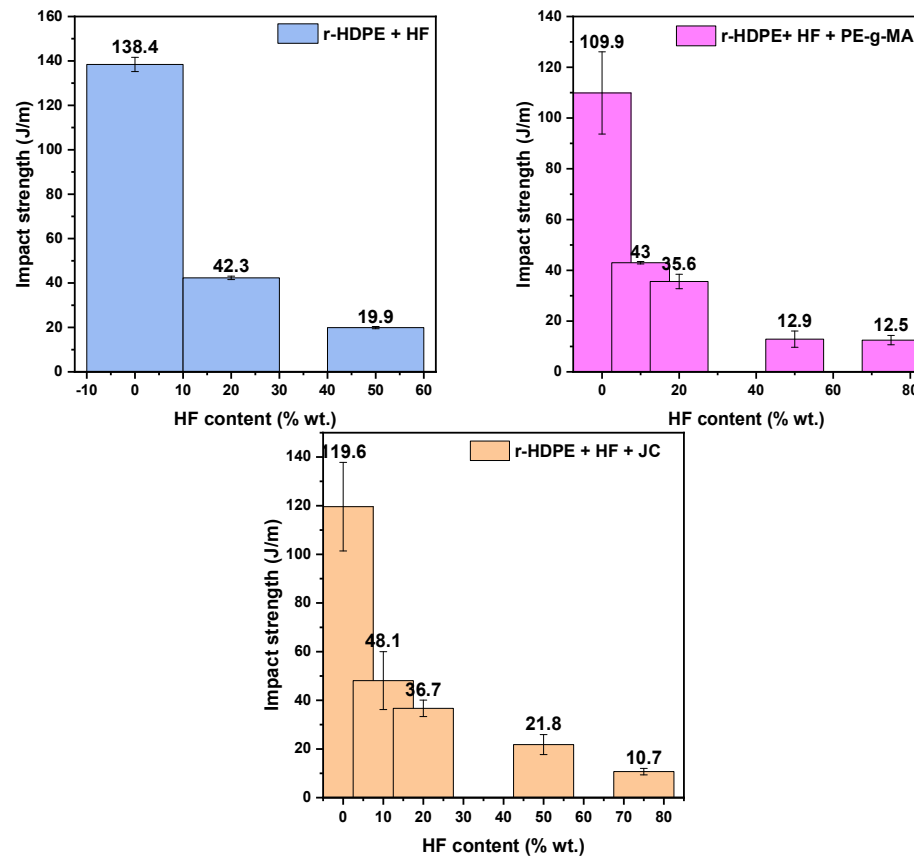


Figure 14. Impact strength of recycled high-density polyethylene (r-HDPE) + hemp fibers (HF) composite materials, with Joncryl (JC) or polyethylene-grafted maleic anhydride (PE-g-MA).

3.9. Antioxidant Activity

Hemp fibers are considered to exhibit significant antioxidant behavior; the antioxidant properties of the r-HDPE + HF samples add valuable information about their further application. Herein, the antioxidant activity of the composites was evaluated by monitoring the reduction in the DPPH radical (DPPH•). Figure 15 illustrates the antioxidant activity over time for different r-HDPE + HF composites immersed in a DPPH/ethanol solution. For the curves presented in Figure 15a, it can be considered that the addition of hemp fibers enhanced the antioxidant activity of the composites over time. Promising are the results for the composite with the higher content of filler (r-HDPE + 75% wt. HF + JC) depicted in Figure 15b, where the residual DPPH• content reached 15.5% after 40 min, showing significant antioxidant activity after only a short period of immersion. Concerning the composite materials with the addition of PE-g-MA, the antioxidant capacity is presented in Figure 15c,d. As it can be observed, the augmentation of the filler led to an increased value of the antioxidant activity.

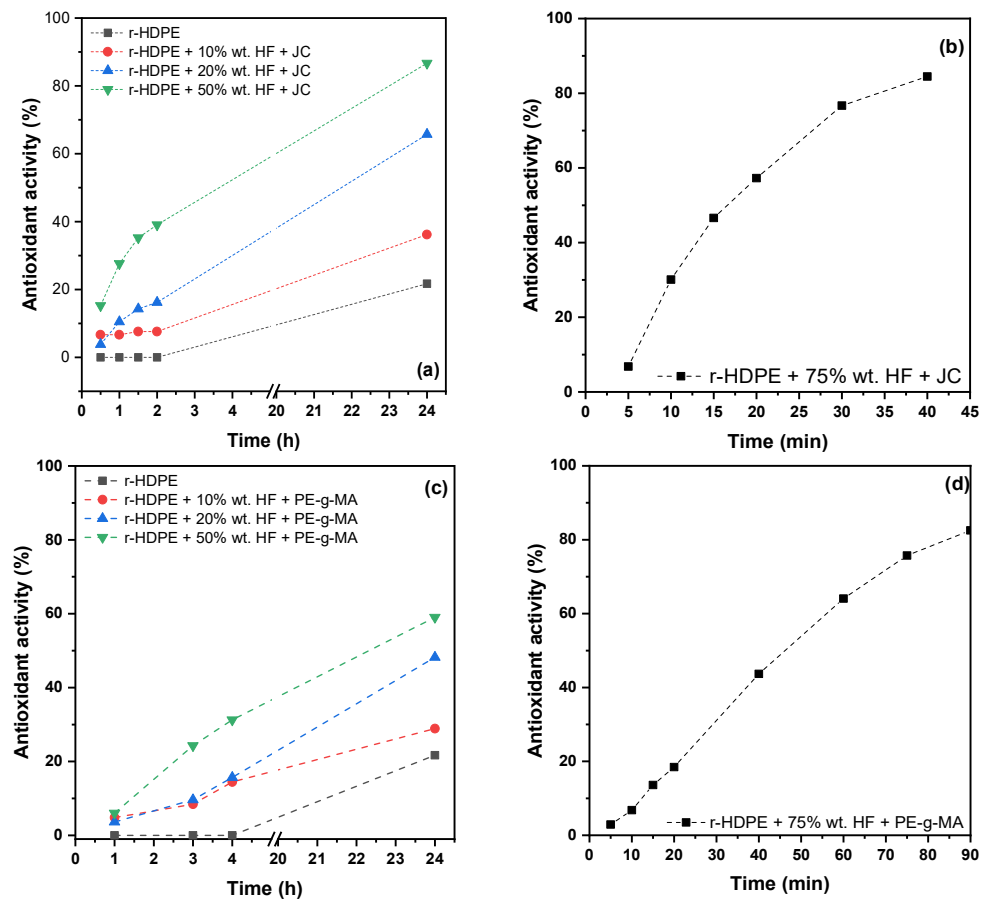


Figure 15. Antioxidant activity of (a) recycled high-density polyethylene (r-HDPE) + 10–50% wt. hemp fibers (HF) + Joncryl (JC), (b) r-HDPE + 75% wt. HF + JC (c) r-HDPE + 10–50% wt. HF + polyethylene-grafted maleic anhydride (PE-g-MA), and (d) r-HDPE + 75% wt. HF + PE-g-MA composite films in DPPH/ethanol solution.

3.10. Soil Degradation

In a final step, soil degradation was performed in order to evaluate the effect of a natural environment on the degradation of the composites, without the presence of enzymes or composting materials, since hemp fibers do not have groups, which could be hydrolyzed from lipases. As it can be observed in Figure 16, neat r-HDPE exhibited a small weight loss due to its low degradation rate. Nevertheless, the presence of hemp fibers increased the degradation rate of the composites compared with neat r-HDPE. Additionally, it could be noted that as the filler concentration increased, the rate of degradation also increased [67]. The latter fact can be attributed to the beginning of microbial degradation of the cellulosic chains of the fibers [51]. As the filler content increased, the moisture absorption and swelling also increased and thus led to faster degradation. Finally, regarding the compatibilizer used, it can be seen that the presence of PE-g-MA led to a higher degradation rate.

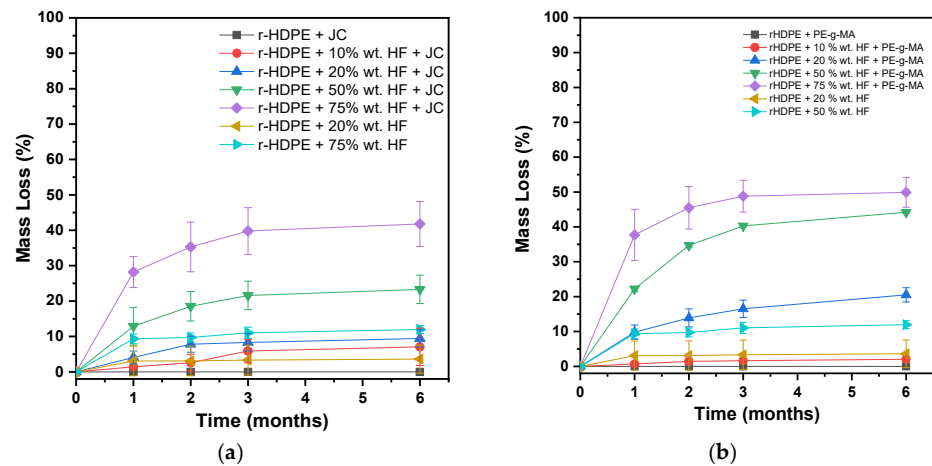


Figure 16. Mass loss versus time plot during soil degradation of the (a) recycled high-density polyethylene (r-HDPE) + hemp fibers (HF) + Joncryl (JC), and (b) r-HDPE + HF + polyethylene-grafted maleic anhydride (PE-g-MA) composites.

4. Conclusions

In this work, eco-friendly hemp-fiber-reinforced recycled HDPE composites were successfully prepared by melt mixing. This process proved satisfactory in providing adequate dispersion of the fillers in the polymer matrix and appropriate to prepare materials with filler concentrations up to 75% wt. It is noteworthy that despite the important hemp fiber content—which, to the best of our knowledge, is the highest found in the literature—the composites obtained with 75% of fibers were not particularly brittle or friable and could be manipulated without losing their structural integrity. Overall, the use of compatibilizers had a beneficial effect on the properties of the composites and our results indicate that better adhesion was achieved with JC compared to PE-g-MA. Regarding the effect of fillers on the crystallization of composites, the effect of the hemp fibers is complex. Low fiber contents seem to facilitate crystallization, while higher contents disrupt the HDPE chain arrangements. However, the overall impact of hemp fibers on melting and crystallization temperatures is rather limited. Regarding the thermal stability of the composites, although the incorporation of hemp fibers results in a decrease in thermal stability, the onset of thermal degradation remains largely higher than the melting temperature of the composites; therefore, the processing of the composites will not be affected by this reduction. Lignin-containing fillers can bring antioxidant activity when incorporated in polymer matrices due to the abundant phenolic hydroxyl groups. Antioxidant properties can contribute to delaying oxidative degradation of the polymeric matrix, thus protecting the composite during thermal treatments and prolonging the life cycle of the composites. Antioxidant measurement indicated the exceptional antioxidant activity of the composites. The composites described in the present work are intended to replace wood/plastic composites which are often used in exterior applications. In this context, the inherent radical scavenging activity of the composites could be beneficial regarding the ageing of the products. Finally, the influence of the fibers on the rate of degradation during soil burial was advantageous; indeed, the presence of the filler significantly reduced the time required for the composite to degrade. Overall, environmentally friendly composites with important biobased content were prepared. The materials displayed interesting features and can be envisaged as green alternatives to conventional WPC products. Future applications could include ornamental objects, as the composites present a nice appearance. Additionally, HDPE is used as a packaging material; therefore, after complementary studies, the composites could find applications in active packaging.

Supplementary Materials: The following supporting information can be downloaded at: <https://www.mdpi.com/article/10.3390/jcs7040138/s1>, Figure S1: Stress–strain curves of (a) r-HDPE, (b) r-HDPE + HF, (c) r-HDPE + HF + JC, and (d) r-HDPE + HF + PE-g-MA composite materials; Table S1: Values of characteristic parameters of r-HDPE + HF composite materials; Table S2: Values of characteristic parameters of r-HDPE + HF + JC composite materials; Table S3: Values of characteristic parameters of r-HDPE + HF + PE-g-MA composite materials.

Author Contributions: Conceptualization, D.N.B.; Validation, formal analysis, and investigation, E.X., I.C., P.P., and A.Z.; Resources, D.N.B.; Writing—original draft, E.X.; Writing—review and editing, E.X., A.Z., and D.N.B.; Supervision, A.Z. and D.N.B. All authors have read and agreed to the published version of the manuscript.

Funding: This research was co-financed by the European Union and Greek national funds through the Operational Program Competitiveness, Entrepreneurship, and Innovation, under the call RESEARCH-CREATE-INNOVATE (project code: T2EDK-00008).

Data Availability Statement: All the data of this study are included in the manuscript and Supplementary Materials.

Acknowledgments: The authors would like to express their gratitude to Eleni Pavlidou, School of Physics, ATh, and Chrysanthi Papoulia, School of Physics, ATh, for the SEM observations. Moreover, they would like to thank Lamprini Malletzidou for conducting the FTIR measurements.

Conflicts of Interest: The authors declare no conflict of interest.

References

1. Rebelein, A.; Int-Veen, I.; Kammann, U.; Scharsack, J.P. Microplastic fibers—Underestimated threat to aquatic organisms? *Sci. Total. Environ.* **2021**, *777*, 146045. [[CrossRef](#)] [[PubMed](#)]
2. Avio, C.G.; Gorbi, S.; Regoli, F. Plastics and microplastics in the oceans: From emerging pollutants to emerged threat. *Mar. Environ. Res.* **2017**, *128*, 2–11. [[CrossRef](#)]
3. Geyer, R.; Jambeck, J.R.; Law, K.L. Production, use, and fate of all plastics ever made. *Sci. Adv.* **2017**, *3*, e1700782. [[CrossRef](#)]
4. Roy, P.; Mohanty, A.K.; Wagner, A.; Sharif, S.; Khalil, H.; Misra, M. Impacts of COVID-19 Outbreak on the Municipal Solid Waste Management: Now and beyond the Pandemic. *ACS Environ. Au* **2021**, *1*, 32–45. [[CrossRef](#)]
5. Prata, J.C.; Silva, A.L.; Walker, T.R.; Duarte, A.C.; Rocha-Santos, T. COVID-19 Pandemic Repercussions on the Use and Management of Plastics. *Environ. Sci. Technol.* **2020**, *54*, 7760–7765. [[CrossRef](#)] [[PubMed](#)]
6. Chrysafi, I.; Asimakidou, T.; Michailidou, G.; Xanthopoulou, E.; Tziamtzi, C.K.; Zamboulis, A.; Bikiaris, D.N. Characterization of the Thermal, Structural, and Mechanical Properties of Recycled HDPE. *Macromol. Symp.* **2022**, *405*, 10–12. [[CrossRef](#)]
7. European Commission. *A New Bioeconomy Strategy for a Sustainable Europe: Restoring Healthy Ecosystems and Enhancing Biodiversity*; European Commission: Brussels, Belgium, 2018.
8. European Commission. *A Sustainable Bioeconomy for Europe: Strengthening the Connection between Economy, Society and the Environment Updated Bioeconomy Strategy*; Publications Office of the European Union: Luxembourg, 2018; pp. 1–107. [[CrossRef](#)]
9. Balu, R.; Dutta, N.K.; Choudhury, N.R. Plastic Waste Upcycling: A Sustainable Solution for Waste Management, Product Development, and Circular Economy. *Polymers* **2022**, *14*, 4788. [[CrossRef](#)]
10. Jung, H.; Shin, G.; Kwak, H.; Hao, L.T.; Jegal, J.; Kim, H.J.; Jeon, H.; Park, J.; Oh, D.X. Review of polymer technologies for improving the recycling and upcycling efficiency of plastic waste. *Chemosphere* **2023**, *320*, 138089. [[CrossRef](#)]
11. Ahmad, F.; Choi, H.S.; Park, M.K. A Review: Natural Fiber Composites Selection in View of Mechanical, Light Weight, and Economic Properties. *Macromol. Mater. Eng.* **2014**, *300*, 10–24. [[CrossRef](#)]
12. Maithil, P.; Gupta, P.; Chandravanshi, M.L. Study of mechanical properties of the natural-synthetic fiber reinforced polymer matrix composite. *Mater. Today Proc.* **2023**. [[CrossRef](#)]
13. Haris, N.I.N.; Hassan, M.Z.; Ilyas, R.; Suhot, M.A.; Sapuan, S.; Dolah, R.; Mohammad, R.; Asyraf, M. Dynamic mechanical properties of natural fiber reinforced hybrid polymer composites: A review. *J. Mater. Res. Technol.* **2022**, *19*, 167–182. [[CrossRef](#)]
14. Parameswaranpillai, J.; Gopi, J.A.; Radoor, S.; Dominic, M.C.; Krishnasamy, S.; Deshmukh, K.; Hameed, N.; Salim, N.V.; Sienkiewicz, N. Turning waste plant fibers into advanced plant fiber reinforced polymer composites: A comprehensive review. *Compos. Part C Open Access* **2023**, *10*, 100333. [[CrossRef](#)]
15. Ilyas, R.; Sapuan, S. The Preparation Methods and Processing of Natural Fibre Bio-polymer Composites. *Curr. Org. Synth.* **2020**, *16*, 1068–1070. [[CrossRef](#)]
16. Jasmin, N.M.; Sathish, S.; Senthil, T.; Naidu, B.A.; Das, A.D.; Arun, K.; Subbiah, R.; Srinivasan, K. Investigation on natural fiber reinforced polymer matrix composite. *Mater. Today Proc.* **2023**, *74*, 60–63. [[CrossRef](#)]
17. Summerscales, J.; Dissanayake, N.P.; Virk, A.S.; Hall, W. A review of bast fibres and their composites. Part 1—Fibres as reinforcements. *Compos. Part A Appl. Sci. Manuf.* **2010**, *41*, 1329–1335. [[CrossRef](#)]

18. Sadrmanesh, V.; Chen, Y. Bast fibres: Structure, processing, properties, and applications. *Int. Mater. Rev.* **2018**, *64*, 381–406. [[CrossRef](#)]
19. Matzinos, P.; Bikiaris, D.N.; Kokkou, S.; Panayiotou, C. Processing and Characterization of LDPE/Starch Products. *J. Appl. Polym. Sci.* **2001**, *79*, 2548–2557. [[CrossRef](#)]
20. Prinós, J.; Bikiaris, D.; Theologidis, S.; Panayiotou, C. Preparation and characterization of LDPE/starch blends containing ethylene/vinyl acetate copolymer as compatibilizer. *Polym. Eng. Sci.* **1998**, *38*, 954–964. [[CrossRef](#)]
21. Väisänen, T.; Das, O.; Tomppo, L. A review on new bio-based constituents for natural fiber-polymer composites. *J. Clean. Prod.* **2017**, *149*, 582–596. [[CrossRef](#)]
22. Yano, H.; Fu, W. Hemp: A Sustainable Plant with High Industrial Value in Food Processing. *Foods* **2023**, *12*, 651. [[CrossRef](#)]
23. Ahmed, A.T.M.F.; Islam, Z.; Mahmud, S.; Sarker, E.; Islam, R. Hemp as a potential raw material toward a sustainable world: A review. *Heliyon* **2022**, *8*, e08753. [[CrossRef](#)]
24. Väisänen, T.; Batello, P.; Lappalainen, R.; Tomppo, L. Modification of hemp fibers (*Cannabis Sativa* L.) for composite applications. *Ind. Crop. Prod.* **2018**, *111*, 422–429. [[CrossRef](#)]
25. Väisänen, T.; Haapala, A.; Lappalainen, R.; Tomppo, L. Utilization of agricultural and forest industry waste and residues in natural fiber-polymer composites: A review. *Waste Manag.* **2016**, *54*, 62–73. [[CrossRef](#)]
26. Liao, J.; Zhang, S.; Tang, X. Sound Absorption of Hemp Fibers (*Cannabis sativa* L.) Based Nonwoven Fabrics and Composites: A Review. *J. Nat. Fibers* **2020**, *19*, 1297–1309. [[CrossRef](#)]
27. Deshmukh, G.S. Advancement in hemp fibre polymer composites: A comprehensive review. *J. Polym. Eng.* **2022**, *42*, 575–598. [[CrossRef](#)]
28. Tutek, K.; Masek, A. Hemp and Its Derivatives as a Universal Industrial Raw Material (with Particular Emphasis on the Polymer Industry)—A Review. *Materials* **2022**, *15*, 2565. [[CrossRef](#)]
29. Dahal, R.K.; Acharya, B.; Dutta, A. Mechanical, Thermal, and Acoustic Properties of Hemp and Biocomposite Materials: A Review. *J. Compos. Sci.* **2022**, *6*, 373. [[CrossRef](#)]
30. Shahzad, A. Hemp fiber and its composites—A review. *J. Compos. Mater.* **2011**, *46*, 973–986. [[CrossRef](#)]
31. Srikavi, A.; Mekala, M. Characterization of Sunn hemp fibers as a substitute for synthetic fibers in composites and various applications. *Ind. Crop. Prod.* **2023**, *192*, 116135. [[CrossRef](#)]
32. Leoni, M.; Musio, S.; Croci, M.; Tang, K.; Magagnini, G.M.; Thouminot, C.; Müssig, J.; Amaducci, S. The effect of agronomic management of hemp (*Cannabis sativa* L.) on stem processing and fibre quality. *Ind. Crop. Prod.* **2022**, *188*, 115520. [[CrossRef](#)]
33. Terzopoulou, Z.N.; Papageorgiou, G.Z.; Papadopoulou, E.; Athanassiadou, E.; Reinders, M.; Bikiaris, D.N. Development and study of fully biodegradable composite materials based on poly(butylene succinate) and hemp fibers or hemp shives. *Polym. Compos.* **2014**, *37*, 407–421. [[CrossRef](#)]
34. Kim, B.-J.; Byun, J.-H.; Park, S.-J. Effects of Graphenes/CNTs Co-reinforcement on Electrical and Mechanical Properties of HDPE Matrix Nanocomposites. *Bull. Korean Chem. Soc.* **2010**, *31*, 2261–2264. [[CrossRef](#)]
35. Kumar P, S.; Jayanarayanan, K.; Balachandran, M. Thermal and Mechanical Behavior of Functionalized MWCNT Reinforced Epoxy Carbon Fabric Composites. *Mater. Today Proc.* **2020**, *24*, 1157–1166. [[CrossRef](#)]
36. Kumar P, S.; Jayanarayanan, K.; Balachandran, M. High-performance thermoplastic polyaryletherketone/carbon fiber composites: Comparison of plasma, carbon nanotubes/graphene nano-anchoring, surface oxidation techniques for enhanced interface adhesion and properties. *Compos. Part B Eng.* **2023**, *253*, 110560. [[CrossRef](#)]
37. Madueke, C.I.; Mbah, O.M.; Umunakwe, R. A review on the limitations of natural fibres and natural fibre composites with emphasis on tensile strength using coir as a case study. *Polym. Bull.* **2022**, *80*, 3489–3506. [[CrossRef](#)] [[PubMed](#)]
38. Lu, N.; Oza, S. A comparative study of the mechanical properties of hemp fiber with virgin and recycled high density polyethylene matrix. *Compos. Part B Eng.* **2013**, *45*, 1651–1656. [[CrossRef](#)]
39. Lu, N.; Oza, S. Thermal stability and thermo-mechanical properties of hemp-high density polyethylene composites: Effect of two different chemical modifications. *Compos. Part B Eng.* **2013**, *44*, 484–490. [[CrossRef](#)]
40. Chimeni-Yomeni, D.; Faye, A.; Rodrigue, D.; Dubois, C. Behavior of polyethylene composites based on hemp fibers treated by surface-initiated catalytic polymerization. *Polym. Compos.* **2021**, *42*, 2334–2348. [[CrossRef](#)]
41. Chimeni, D.Y.; Dubois, C.; Rodrigue, D. Polymerization compounding of hemp fibers to improve the mechanical properties of linear medium density polyethylene composites. *Polym. Compos.* **2017**, *39*, 2860–2870. [[CrossRef](#)]
42. Lu, N.; Swan, R.H., Jr.; Ferguson, I. Composition, structure, and mechanical properties of hemp fiber reinforced composite with recycled high-density polyethylene matrix. *J. Compos. Mater.* **2012**, *46*, 1915–1924. [[CrossRef](#)]
43. Angulo, C.; Brahma, S.; Espinosa-Dzib, A.; Peters, R.; Stewart, K.M.E.; Pillay, S.; Ning, H. Development of hemp fiber composites with recycled high density polyethylene grocery bags. *Environ. Prog. Sustain. Energy* **2021**, *40*, e13617. [[CrossRef](#)]
44. Amiandamhen, S.O.; Meincken, M.; Tyhoda, L. Natural Fibre Modification and Its Influence on Fibre-matrix Interfacial Properties in Biocomposite Materials. *Fibers Polym.* **2020**, *21*, 677–689. [[CrossRef](#)]
45. Tanasă, F.; Zănoagă, M.; Teacă, C.; Nechifor, M.; Shahzad, A. Modified hemp fibers intended for fiber-reinforced polymer composites used in structural applications—A review. I. Methods of modification. *Polym. Compos.* **2019**, *41*, 5–31. [[CrossRef](#)]
46. Liu, M.; Thygesen, A.; Summerscales, J.; Meyer, A.S. Targeted pre-treatment of hemp bast fibres for optimal performance in biocomposite materials: A review. *Ind. Crop. Prod.* **2017**, *108*, 660–683. [[CrossRef](#)]

47. Graziano, A.; Jaffer, S.; Sain, M. Review on modification strategies of polyethylene / polypropylene immiscible thermoplastic polymer blends for enhancing their mechanical behavior. *J. Elastomers Plast.* **2018**, *54*, 291–336. [[CrossRef](#)]
48. Karaagac, E.; Koch, T.; Archodoulaki, V.-M. Choosing an Effective Compatibilizer for a Virgin HDPE Rich-HDPE/PP Model Blend. *Polymers* **2021**, *13*, 3567. [[CrossRef](#)] [[PubMed](#)]
49. Utracki, L.A. Compatibilization of Polymer Blends. *Can. J. Chem. Eng.* **2002**, *80*, 1008–1016. [[CrossRef](#)]
50. Andre, J.S.; Li, B.; Chen, X.; Paradkar, R.; Walther, B.; Feng, C.; Tucker, C.; Mohler, C.; Chen, Z. Interfacial reaction of a maleic anhydride grafted polyolefin with ethylene vinyl alcohol copolymer at the buried solid/solid interface. *Polymer* **2021**, *212*, 123141. [[CrossRef](#)]
51. Roumeli, E.; Terzopoulou, Z.; Pavlidou, E.; Chrissafis, K.; Papadopoulou, E.; Athanasiadou, E.; Triantafyllidis, K.; Bikiaris, D.N. Effect of maleic anhydride on the mechanical and thermal properties of hemp/high-density polyethylene green composites. *J. Therm. Anal. Calorim.* **2015**, *121*, 93–105. [[CrossRef](#)]
52. Wang, Y.; Shi, Y.; Shao, W.; Ren, Y.; Dong, W.; Zhang, F.; Liu, L.-Z. Crystallization, Structures, and Properties of Different Polyolefins with Similar Grafting Degree of Maleic Anhydride. *Polymers* **2020**, *12*, 675. [[CrossRef](#)]
53. Naik, J.B.; Mishra, S. Esterification effect of maleic anhydride on swelling properties of natural fiber/high density polyethylene composites. *J. Appl. Polym. Sci.* **2007**, *106*, 2571–2574. [[CrossRef](#)]
54. Chimeni, D.Y.; Toupe, J.L.; Dubois, C.; Rodrigue, D. Effect of surface modification on the interface quality between hemp and linear medium-density polyethylene. *J. Appl. Polym. Sci.* **2016**, *133*, 1–10. [[CrossRef](#)]
55. Standau, T.; Nofar, M.; Dörr, D.; Ruckdäschel, H.; Altstädt, V. A Review on Multifunctional Epoxy-Based Joncryl® ADR Chain Extended Thermoplastics. *Polym. Rev.* **2021**, *62*, 296–350. [[CrossRef](#)]
56. Grigora, M.-E.; Terzopoulou, Z.; Tsongas, K.; Klonos, P.; Kalafatakis, N.; Bikiaris, D.; Kyritsis, A.; Tzetzis, D. Influence of Reactive Chain Extension on the Properties of 3D Printed Poly(Lactic Acid) Constructs. *Polymers* **2021**, *13*, 1381. [[CrossRef](#)]
57. Venkatesan, K.B.; Karkhanis, S.S.; Matuana, L.M. Microcellular foaming of poly(lactic acid) branched with food-grade chain extenders. *J. Appl. Polym. Sci.* **2021**, *138*, 50686. [[CrossRef](#)]
58. Tucci, F.; Vedernikov, A. Design Criteria for Pultruded Structural Elements. In *Reference Module in Materials Science and Materials Engineering*; Elsevier, B.V., Ed.; Academic Press: Amsterdam, The Netherlands, 2021; pp. 51–58.
59. Minchenkov, K.; Vedernikov, A.; Safonov, A.; Akhatov, I. Thermoplastic Pultrusion: A Review. *Polymers* **2021**, *13*, 180. [[CrossRef](#)]
60. Cassagnau, P.; Bounor-Legaré, V.; Fenouillot, F. Reactive Processing of Thermoplastic Polymers: A Review of the Fundamental Aspects. *Int. Polym. Process* **2007**, *22*, 218–258. [[CrossRef](#)]
61. Blois, M.S. Antioxidant Determinations by the Use of a Stable Free Radical. *Nature* **1958**, *181*, 1199–1200. [[CrossRef](#)]
62. Gulmine, J.; Janissek, P.; Heise, H.; Akcelrud, L. Polyethylene characterization by FTIR. *Polym. Test.* **2002**, *21*, 557–563. [[CrossRef](#)]
63. Mouallif, I.; Latrach, A.; Chergui, M.; Benali, A.; Barbe, N. FTIR study of HDPE structural changes, moisture absorption and mechanical properties variation when exposed to sulphuric acid aging in various temperatures. *Mater. Sci.* **2011**, 1–7.
64. Krehula, L.K.; Katančić, Z.; Siročić, A.P.; Hrnjak-Murgić, Z. Weathering of High-Density Polyethylene-Wood Plastic Composites. *J. Wood Chem. Technol.* **2013**, *34*, 39–54. [[CrossRef](#)]
65. Neves, A.C.C.; Rohen, L.A.; Mantovani, D.P.; Carvalho, J.P.R.G.; Vieira, C.M.F.; Lopes, F.P.D.; Simonassi, N.T.; da Luz, F.S.; Monteiro, S.N. Comparative mechanical properties between biocomposites of Epoxy and polyester matrices reinforced by hemp fiber. *J. Mater. Res. Technol.* **2020**, *9*, 1296–1304. [[CrossRef](#)]
66. Dolça, C.; Fages, E.; Gong, E.; Garcia-Sanoguera, D.; Balart, R.; Quiles-Carrillo, L. The Effect of Varying the Amount of Short Hemp Fibers on Mechanical and Thermal Properties of Wood-Plastic Composites from Biobased Polyethylene Processed by Injection Molding. *Polymers* **2021**, *14*, 138. [[CrossRef](#)] [[PubMed](#)]
67. Bikiaris, D.; Prinos, J.; Panayiotou, C. Effect of EAA and starch on the thermooxidative degradation of LDPE. *Polym. Degrad. Stab.* **1997**, *56*, 1–9. [[CrossRef](#)]

Disclaimer/Publisher’s Note: The statements, opinions and data contained in all publications are solely those of the individual author(s) and contributor(s) and not of MDPI and/or the editor(s). MDPI and/or the editor(s) disclaim responsibility for any injury to people or property resulting from any ideas, methods, instructions or products referred to in the content.